Measurement and Discussion of Inductance Distortion caused by Magnetic Saturation for Sensorless Control of IPMSM

Yang Zhao, Bunpei Naito, Shinji Doki and Shigeru Okuma
Department of Electrical Engineering and Computer Science
Nagoya University, Aichi, Japan 464-8603
Telephone: +81-52-789-2777
Fax: +81-52-789-3140
Email: zhao@okuma.nuee.nagoya-u.ac.jp, naito@okuma.nuee.nagoya-u.ac.jp, doki@nagoya-u.jp, okuma@nagoya-u.jp

***Abstract*—This paper considers the inductance spatial distribution of Interior Permanent Magnetic Synchronous Motors (IPMSM) in various load conditions. The IPMSM machine possess a unique relationship between phase inductance and rotor position, that make it possible to implement sensorless control by extracting rotor position information from the inductance distribution. During the past two decades, many sensorless control methods for IPMSM drive based on magnetic saliency have been proposed. However, the inductance varies with the load conditions and the motor structure, which causes the sensorless control performance to be degraded. This paper reports on a high-frequency voltage signal injection method of measuring the phase inductance, and focuses discussion on the inductance spatial distribution including magnetic saturation.**

I. Introduction

IPMSM machine have several advantages such as high efficiency and high torque density. For high performance of IPMSM drive, the rotor position is required, which is usually detected by mechanical position sensor. Because it is recognized that position sensors are expensive and mechanically unreliable, up to now many sensorless control methods for IPMSM drive are proposed [1]-[6].

For applications that require IPMSM working at low speed or standstill, high frequency signal injection methods have been developed. These techniques measure the response of phase current according to the additional excitation, in order to calculate phase inductance. The value of phase inductance is assumed to be a sinusoidal function of rotor position. Therefore, the rotor position can be derived form the inductance.

However, the needs of IPMSM machine that possess higher torque density and shorter motor length, have increased recently, such as the application in a hybrid vehicles. In these cases, the influence of permanent magnetic flux variation and magnetic saturation must be taken into consideration [2]. As the first step in our research on sensorless control of IPMSM considering magnetic saturation, This paper will measure and discuss the inductance spatial distribution at various load conditions in order to evaluate the undesired distortion in inductance, and propose a new sensorless control scheme using pattern matching technique. Experimental results suggest that it might be capable of improving the performance of IPMSM sensorless control by taking the magnetic saturation discussed in this paper into consideration.

II. Inductance Measurement Method

Consider the injection of high frequency pulse voltage signal via the inverter in the manner of [1], the phase inductance can be acquired by measuring the response of the phase current, and then the rotor position information can be derived from the inductance distribution.

The idealized phase current variation of the test motor is shown in Fig.1. In this paper, we apply a method only using single phase for the injection of high frequency voltage signal in synchronism with the PWM operation. Based on the space vectors as defined in Fig.2, the switching patterns resulting from the above described additional excitation can be classified as follows:

(1) Arm of phase u is turned on (voltage vector V1).
(2) Arms of phase v and w are turned on (voltage vector V4).
(3) Arms of all three phase are turned on or off (voltage vector V0 or V7).

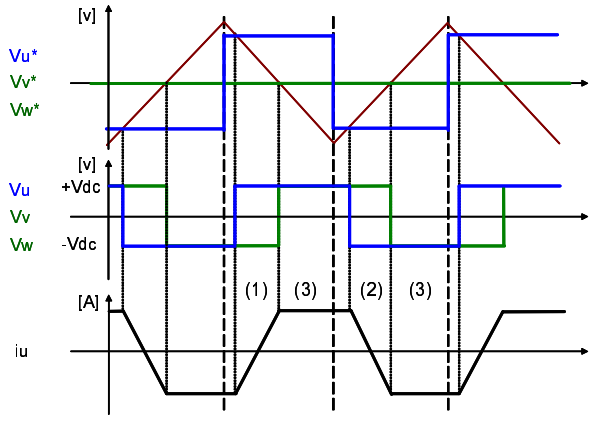

Fig. 1. Idealized current response to single phase injection of pulse voltage

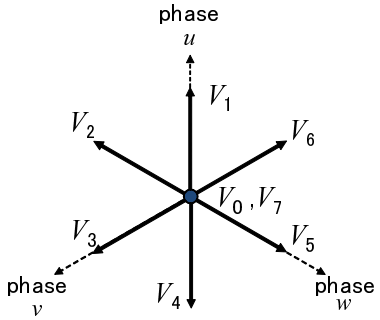

Fig. 2. Space voltage vectors of the inverter

As shown in Fig.1, the phase current rises during the rising inductance period when a positive torque is applied and, it flows in the opposite direction during the decreasing inductance period when a negative torque is applied. The derivative of phase current occurs within rising inductance period and decreasing inductance period, is detected for inductance calculation.

The phase voltage equation of IPMSM is usually established as

$$\begin{bmatrix} v_u \\ v_v \\ v_w \end{bmatrix} = \begin{bmatrix} pL_u & pM_{uv} & pM_{wu} \\ pM_{uv} & pL_v & pM_{vw} \\ pM_{wu} & pM_{vw} & pL_w \end{bmatrix} \begin{bmatrix} i_u \\ i_v \\ i_w \end{bmatrix} \quad (1)$$

where v, i, L, M denote the phase voltage, phase current, phase inductance, and the mutual inductance, respectively. Because our research interests focus on sensorless control operating at low speed and standstill based on high frequency signal injection method, the phase resistance R and rotor angular speed ω are negligible.

To better understand the behavior of the current seen in Fig.1, assume the case that the arm of phase u is turned ON. In this case, the fundamental motor voltage equation expression is given as

$$\begin{bmatrix} \frac{2}{3}V_{dc} \\ -\frac{1}{3}V_{dc} \\ -\frac{1}{3}V_{dc} \end{bmatrix} = \begin{bmatrix} pL_u & pM_{uv} & pM_{wu} \\ pM_{uv} & pL_v & pM_{vw} \\ pM_{wu} & pM_{vw} & pL_w \end{bmatrix} \begin{bmatrix} i_u \\ -\frac{i_u}{2} \\ -\frac{i_u}{2} \end{bmatrix} \quad (2)$$

where V_{dc} is DC link voltage, i_u is the current of phase u, and $i_v = -i_u/2$, $i_w = -i_u/2$.

By transforming (2) to the equation in the stationary reference frame, we have

$$v_\alpha = \sqrt{\frac{2}{3}}(v_u - \frac{1}{2}v_v - \frac{1}{2}v_w) = \sqrt{\frac{2}{3}}V_{dc} \quad (3)$$

$$i_\alpha = \sqrt{\frac{2}{3}}(i_u - \frac{1}{2}i_v - \frac{1}{2}i_w) = \sqrt{\frac{3}{2}}i_u \quad (4)$$

$$v_\beta = \sqrt{\frac{1}{2}}(v_v - v_w) = 0 \quad (5)$$

$$i_\beta = \sqrt{\frac{1}{2}}(i_v - i_w) = 0 \quad (6)$$

$$\begin{bmatrix} \sqrt{\frac{2}{3}}V_{dc} \\ 0 \end{bmatrix} = \begin{bmatrix} pL_\alpha & pL_{\alpha\beta} \\ pL_{\alpha\beta} & pL_\beta \end{bmatrix} \begin{bmatrix} \sqrt{\frac{3}{2}}i_u \\ 0 \end{bmatrix} \quad (7)$$

$$1.5 * L_\alpha = \frac{V_{dc}}{pi_u} \quad (8)$$

where $v_\alpha, v_\beta, i_\alpha, i_\beta, L_\alpha, L_\beta, L_{\alpha\beta}$ are the voltage, current, and inductance value in the stationary reference frame, respectively. In (8), the V_{dc} can be estimate accurately according to the dc link voltage. The di_u/dt term can be obtained by detecting the derivative of the current i_u. Therefore, the inductance L_α can be obtained simply once the dc link voltage and i_u are sampled.

III. Experimental Results

A. Experimental Setup

Fig.3 shows the experimental setup used for the experiments presented in this paper. It consists of a PWM inverter fed eight-pole IPMSM machine, with additional excitation via the inverter. A digital oscilloscope was used to memory the dc link voltage and the phase current resulting from it. These signals were then processed offline in order to calculate the inductance L_α as in (8). For example, Fig.4 shows a phase current response according to the injected excitation which is stored by the digital oscilloscope. The motor parameters are shown in Table I. The amplitude and frequency of the injected voltage signal is shown in Table II.

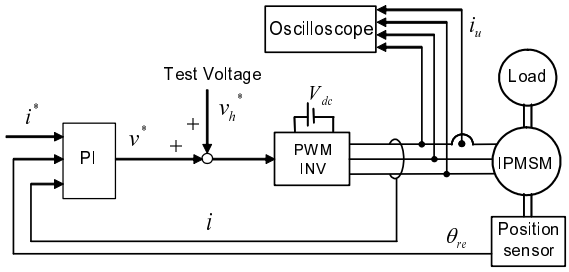

Fig. 3. Block Diagram of Experimental Setup

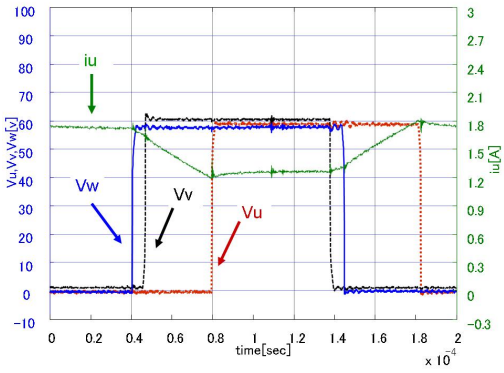

Fig. 4. Current Response to the Test Vector

TABLE I
MOTOR PARAMETERS

Resistance (R)	0.235 [Ω]
d-axis inductance (L_d)	3.0 [mH]
q-axis inductance (L_q)	7.0 [mH]
EMF constant (K_E)	0.13 [V/(rad/s)]
Number of poles	8

TABLE II
CONTROLLER PARAMETERS AND INJECTED SIGNAL

Current sampling rate	5[kHz]
PWM carrier frequeny	5[kHz]
DC-link voltage	60[v]
Injected signal frequency	5[kHz]
Injected signal amplitude	20[v]

B. Experimental Results of L_α

Fig.6 to Fig.16 show the experimental results of L_α for several i_q (torque current) values. The measurement has been performed with respect to each rotor position at standstill condition. Error bars on the graph indicate standard deviation of the values. The motor is controlled by the real rotor position which is detected by a incremental encoder, and the i_d (field current) is controlled to zero by a PI controller whose bandwidth is 2000 rad/s. For comparison, the reference value of L_α which is assumed to have a sinusoidal spatial distribution shown in Fig.6, is calculated as follows:

$$1.5 * L_\alpha = 1.5 * (\frac{L_d + L_q}{2} + \frac{L_d - L_q}{2} * cos2\theta_{re}) \quad (9)$$

where θ_{re} is the rotor position. From the experimental results it can be seen that

(i) L_α is similar to a sinusoidal waveform at low load conditions.
(ii) according to the increase in torque current i_q, the actual waveform of L_α is highly distorted compared with its model (9).
(iii) The average value of estimated L_α decreases according to the increase in i_q.
(iv) The estimated L_α in case of that the arm of phase u is turned on, is different from that when the arms of phase v and w are turned on, even at a same load condition.
(v) A smaller standard deviation of the experimental results can be obtained if the experimental data are processed separately according to the switching pattern resulting from the test voltage vectors.
(vi) Phase shift between the estimated L_α and its model increases when the load applied increases.

From the previous analysis it must be considered that the implementation of sensorless control at heavy load conditions is very difficult due to magnetic saturation that cause the shape of inductance distribution highly distorted from its sinusoidal model, which represents the function relationships between inductance and rotor position.

Furthermore, in case of implementing a sensorless control with mathematical model, as the average value and standard deviation of estimated inductance vary with the switching pattern generated by the injected pulse voltage, relatively accurate estimation of inductance L_α might be obtained by processing experimental data separately according to the different switching pattern than processing all of the data.

IV. A NEW SENSORLESS CONTROL SCHEME USING PATTERN MATCHING METHOD

In the preceding section of this paper, it has been shown that the distribution of inductance is periodic with multiple harmonics, in which the position information is included. In this paper we also present a new method for estimation of rotor position, based on pattern matching technique.

The fundamental inductance equation expression is reviewed as follows:

$$L_{\alpha u} = L_0 + L_1 cos(2\theta_{re}) \quad (10)$$

$$L_{\alpha v} = L_0 + L_1 cos(2\theta_{re} + \frac{2\pi}{3}) \quad (11)$$

$$L_{\alpha w} = L_0 + L_1 cos(2\theta_{re} - \frac{2\pi}{3}) \quad (12)$$

where $L_{\alpha u}$, $L_{\alpha v}$ and $L_{\alpha w}$ are the inductance calculated as well as (8), in u, v and w reference frame, respectively. $L_0 = (L_d + L_q)/2$, $L_1 = (L_d - L_q)/2$. Therefor, the position θ_{re} can be obtained as:

$$\theta_{re} = \frac{1}{2} tan^{-1} \frac{\sqrt{3}(L_{\alpha w} - L_{\alpha v})}{2L_{\alpha u} - L_{\alpha v} - L_{\alpha w}} \quad (13)$$

Equation(13) is used as a reference position estimation of IPMSM in this paper, which can be considered as a representation of conventional sensorless control methods with dependence on sinusoidal distribution of inductance. Obviously, the sensorless control performance can be degraded at heavy load conditions due to the effect of the higher harmonics not considered in (13).

In order to improve the performance of sensorless control drive with pattern matching, an evaluation function approach is used in this paper. Expression for computing the evaluation function is proposed as follows:

$$\begin{aligned} J(\theta_{re}) &= (L_{\alpha u\_on} - L_{\alpha u\_t\_on})^2 \\ &+ (L_{\alpha v\_on} - L_{\alpha v\_t\_on})^2 \\ &+ (L_{\alpha w\_on} - L_{\alpha w\_t\_on})^2 \\ &+ (L_{\alpha u\_off} - L_{\alpha u\_t\_off})^2 \\ &+ (L_{\alpha v\_off} - L_{\alpha v\_t\_off})^2 \\ &+ (L_{\alpha w\_off} - L_{\alpha w\_t\_off})^2 \end{aligned} \quad (14)$$

where $L_{\alpha u\_t\_on}$, $L_{\alpha v\_t\_on}$, $L_{\alpha w\_t\_on}$, $L_{\alpha u\_t\_off}$, $L_{\alpha v\_t\_off}$ and $L_{\alpha w\_t\_off}$ represent a current-inductance-rotor position table, which is constructed by FFT analysis of previously-sampled inductance data. $L_{\alpha u\_on}$, $L_{\alpha v\_on}$, $L_{\alpha w\_on}$, $L_{\alpha u\_off}$, $L_{\alpha v\_off}$ and $L_{\alpha w\_off}$ are the samples according to the switching pattern of PWM operation, when implementing sensorless control. The θ_{re} which minimized the evaluation function will be the result of position estimation.

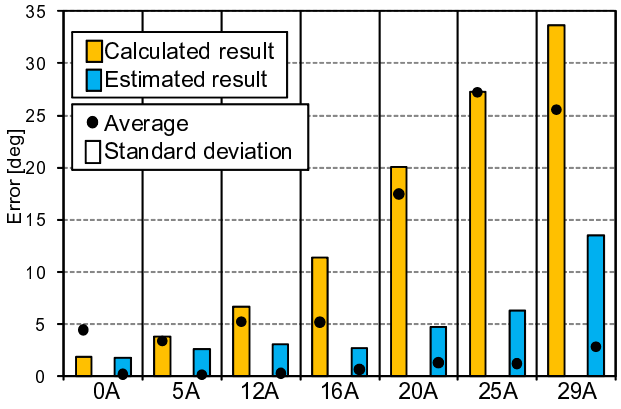

Fig. 5. Estimated and calculated position error at 0 speed

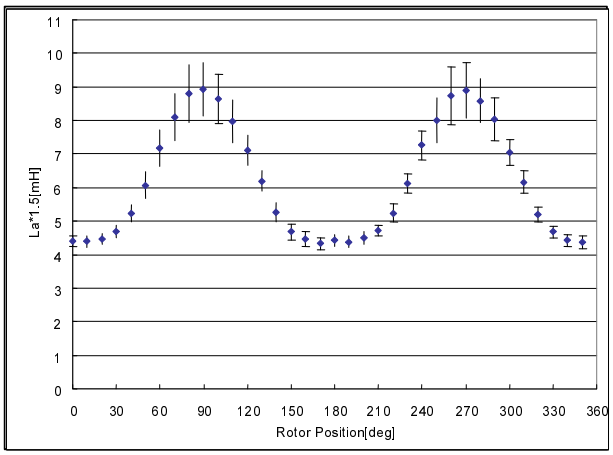

Fig. 8. Average and standard deviation of inductance (id=0, iq=5A)

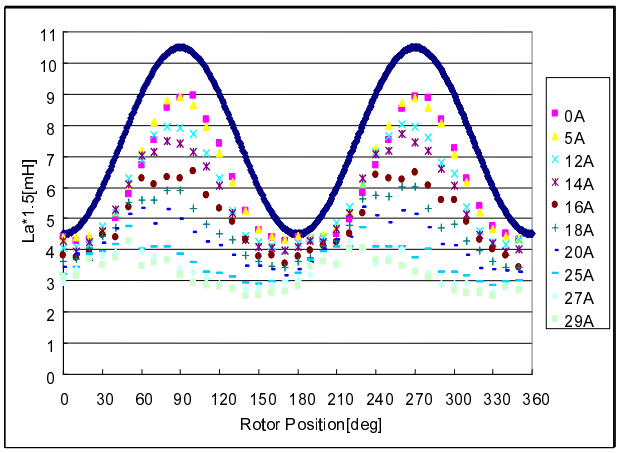

Fig. 6. Idealized current response to single phase injection of test vector

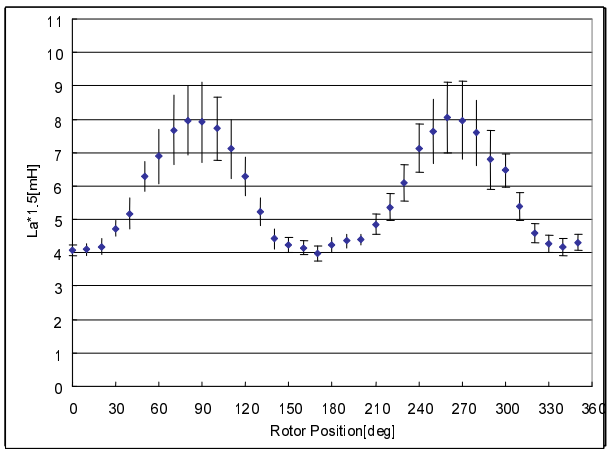

Fig. 9. Average and standard deviation of inductance (id=0, iq=12A)

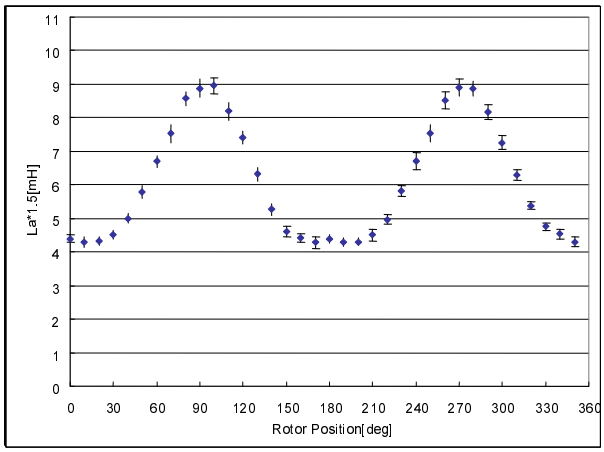

Fig. 7. Average and standard deviation of inductance (id=0, iq=0)

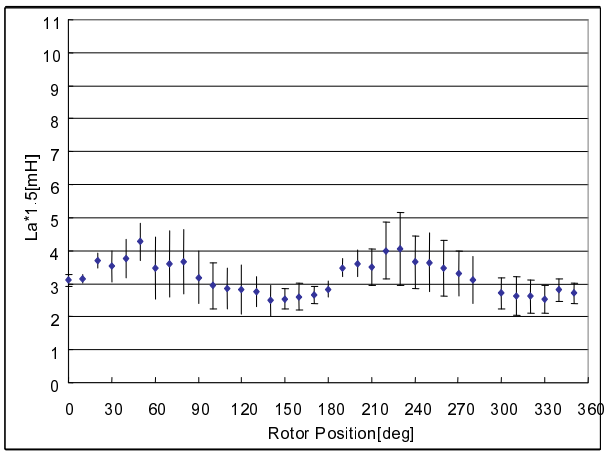

Fig. 10. Average and standard deviation of inductance (id=0, iq=29A)

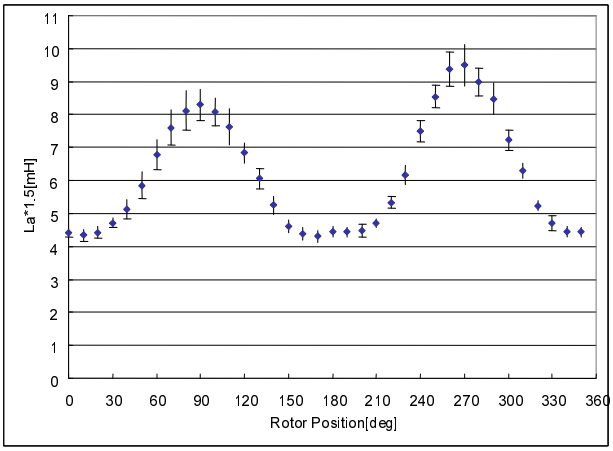

Fig. 11. Average and standard deviation, u phase turned on (id=0, iq=5A)

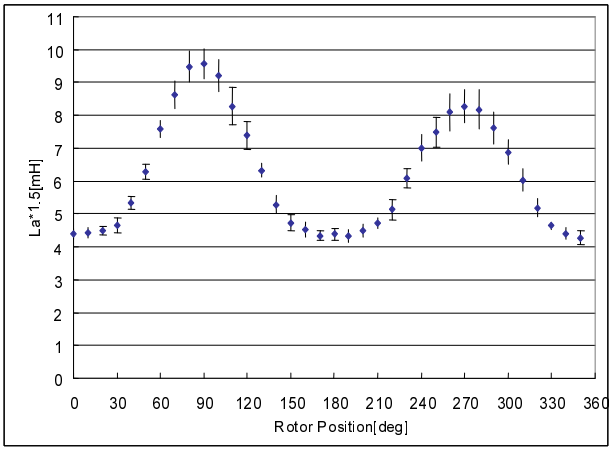

Fig. 12. Average and standard deviation, vw phase turned on (id=0, iq=5A)

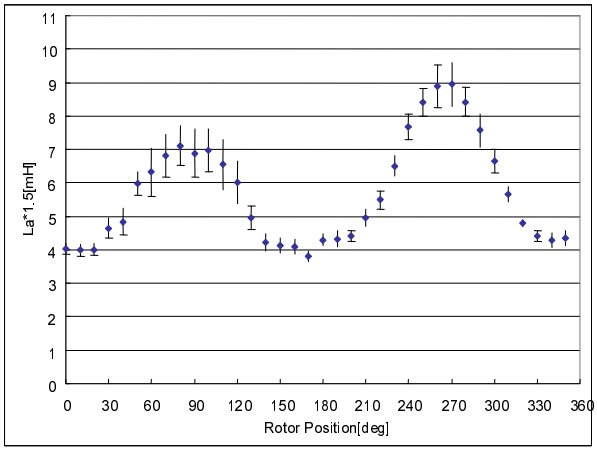

Fig. 13. Average and standard deviation, u phase turned on (id=0, iq=12A)

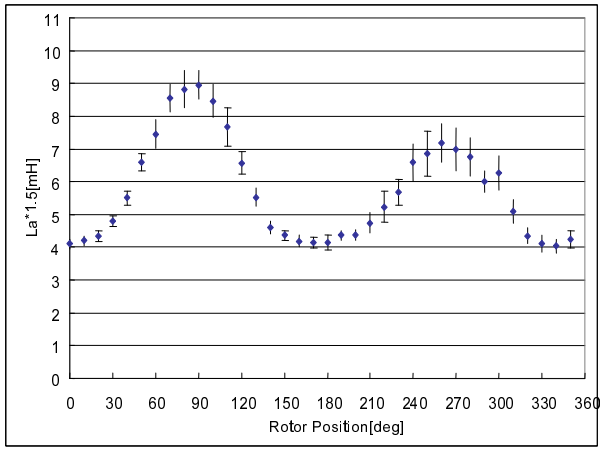

Fig. 14. Average and standard deviation, vw phase turned on (id=0, iq=12A)

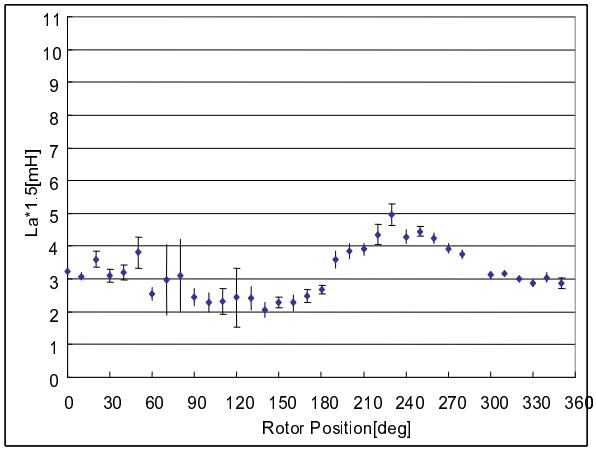

Fig. 15. Average and standard deviation, u phase turned on (id=0, iq=29A)

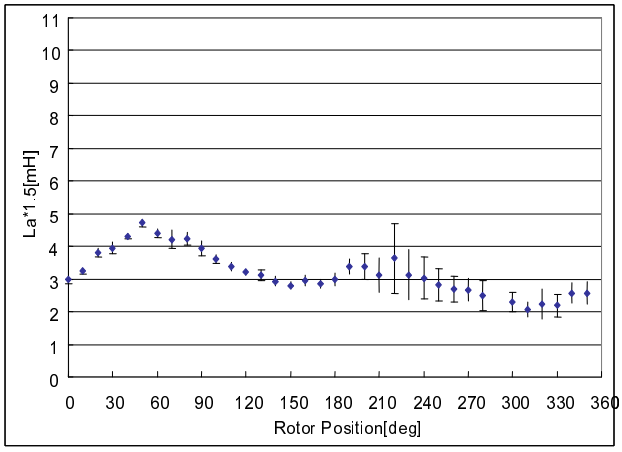

Fig. 16. Average and standard deviation, vw phase turned on (id=0, iq=29A)

The proposed sensorless control scheme is studied on the test motor at standstill. Fig.(5) shows the estimated rotor position error of this method under various load conditions, compared with the calculated values according to (13).

The result demonstrates that the proposed method, which considering the harmonic inductance distribution by using pattern matching, can significantly improves accuracy of position estimation

V. Conclusion

This paper focuses on measurement and discussion of inductance spatial distribution including magnetic saturation. The experimental result shows that the value of measured inductance decreases when the torque current increases, and the phase shift also occurs at the same time. Moreover, the value and standard deviation of experimental results vary with the switching pattern generated by the test vector.

For the magnetic saturation characteristic mentioned above, it can be considered that conventional sensorless technique which assume the inductance distribution as a sinusoidal function of rotor position will not be suitable for implementation at such condition. On the other hand, it suggests the possibility that the performance of sensorless control of IPMSM might be improved by taking the previous analysis into consideration. Further research will be necessary on it.

References

[1] D.Kaneko, Y.Iwaji, K.Sakamoto, T.Endoh, "Initial Rotor Position Estimation of Interior Permanent Magnet Synchronous Motor" (in Japanese), IEEJ Trans.1A,vol.123-D,No.2,2003 pp.140-148 (2003)

[2] N.Imai, S.Morimoto, M.Sanada, Y.Takeda, "Influence of Magnetic Saturation on Sensorless Control for Interior Permanent-Magnet Synchronous Motors With Concentrated Windings", IEEE Trans. Industry Applications, Vol.42, No.5, pp. 1193-1200.

[3] T.Noguchi, K.Motono, "Performance Improvement of Mechanical-Sensorless IPM Motor Drive Using Harmonic Current Injection" (in Japanese), IIEEJ Trans,1A,vol.126-D,No.3,2006 pp.360-367 (2006)

[4] M.J.Corley, R.D.Lorenz, "Rotor position and velocity estimation for a salient-pole permanent-magnet synchronous machine at standstill and high-speeds", IEEE Trans. Industry Applications, Vol.34, No.4, pp. 784-789.

[5] Y.S.Jeong, R.D.Lorenz, T.M.Jahns, S.K.Sul, "Initial Rotor Position Estimation of an Interior Permanent-Magnet Synchronous Machine Using Carrier-Frequency Injection Methods", IEEE Trans. Industry Applications, Vol.41, No.1, pp. 38-45.

[6] R.Leidhold, P.Mutschler, Y.Tong, Y.Takeda, T.Hirasa, "Sensorless Position estimation by using the high frequency zero-sequence generated by the inverter", IECON Proceedings. pp. 1278-1283, 2009.